

# A spectrally tunable plasmonic photosensor with an ultrathin semiconductor region

Shuyuan Xiao · Tao Wang · Xiaoyun Jiang · Boyun Wang · Chen Xu

Received: date / Accepted: date

**Abstract** Surface plasmon resonance (SPR) has been widely utilized to improve the absorption performance in the photosensors. Graphene has emerged as a promising plasmonic material, which supports tunable SPR and shows significant flexibility over metals. In this letter, a hybrid photosensor based on the integration of periodic cross-shaped graphene arrays with an ultrathin light-absorbing semiconductor is proposed. A tenfold absorption enhancement over a large range of the incidence angle for both light polarizations as well as a considerably high photogeneration rate ( $\sim 10^{37}$ ) is demonstrated at the resonance. Compared with traditional metal-based plasmon-enhanced photosensors, the absorption enhancement here can be expediently tuned with manipulating the Fermi energy of graphene. The proposed photosensor can amplify the photoresponse to the incidence light at the selected wavelength and thus be utilized in photosensing with high efficiency and tunable spectral selectivity in the mid-infrared (mid-IR) and terahertz (THz) regime.

**Keywords** Surface plasmons · Graphene optical properties · Photodetectors

---

Shuyuan Xiao · Tao Wang(✉) · Xiaoyun Jiang  
Wuhan National Laboratory for Optoelectronics, Huazhong University of Science and Technology, Wuhan 430074, People's Republic of China  
E-mail: wangtao@hust.edu.cn

Boyun Wang  
School of Physics and Electronic-information Engineering, Hubei Engineering University, Xiaogan 432000, People's Republic of China

Chen Xu  
Department of Physics, New Mexico State University, Las Cruces 88001, United State of America

## 1 Introduction

In recent years, surface plasmon resonance (SPR) has been introduced as an effective approach to reduce the thickness of the light-absorbing semiconductors in the photosensors, while maintaining a sufficient light absorption, leading to highly efficient photogeneration of charge carriers and current collection[1, 2, 3, 4, 5]. The basic physics lies in that the collective electronic excitations at metal/dielectric interface trap the incidence light in the near field, and induce the effects of electromagnetic field enhancement and light energy concentration. In the past, a variety of metal-based plasmonic structures have been proposed to integrate with the light-absorbing semiconductors to improve their absorption performance[6, 7, 8, 9, 10, 11, 12]. Nevertheless, once the metal structures are fabricated, the resonance wavelength and thus the operation range of these hybrid photosensors will be unchangeable, which greatly hamper the flexible applications in practice.

Graphene, a monolayer of carbon atoms arranged in plane with a honeycomb lattice, behaves like metals when interacting with the incidence light and supports SPR for active material applications in the mid-infrared (mid-IR) and terahertz (THz) regime[13, 14, 15, 16]. Furthermore, the continuously tunable surface conductivity of graphene with manipulating its Fermi energy enables actively tunable resonance[17, 18, 19, 20, 21, 22], which can be utilized to enhance the light absorption at the selected wavelength and thus amplify the photoresponse to the incidence light with tunable spectral selectivity[23]. So far tunable absorption enhancement with graphene SPR has been extensively studied, however, most of previous studies concentrated on the absorption enhancement in graphene itself while the utilization of graphene SPR to trap light and enhance the light absorption in other light-absorbing semiconductors is very limited.

To explore this possibility, in this letter, a hybrid photosensor based on the integration of periodic cross-shaped graphene arrays with an ultrathin light-absorbing semiconductor region is numerically studied. The simulation results reveal that the excitations of SPR in the cross-shaped graphene arrays trap a substantial part of the incidence light in the near field and lead to a tenfold absorption enhancement in the surrounding light-absorbing semiconductor. With manipulating the Fermi energy of graphene, the absorption enhancement can be expediently tuned. Compared with the metal-based devices, our proposed photosensor can provide a comparable photogeneration rate and operate over a large spectral range.

## 2 The geometric structure and numerical model

The schematic geometry of our proposed photosensor is illustrated in FIG. 1. The unit cell is arranged in a periodic array with a lattice constant  $P = 400$  nm and composed of a cross-shaped graphene resonator on the top of the light-absorbing semiconductor separated by an insulating spacer. The length

and the width of the cross-shaped graphene resonator are  $L = 240$  nm and  $W = 80$  nm, and the effective thickness is set as  $t_g = 1$  nm. The thicknesses of the insulating spacer and the light-absorbing semiconductor are  $t_i = 20$  nm and  $t_a = 100$  nm, and the substrate is assumed to be semi-infinite. Both the insulating spacer and the substrate are considered as lossless dielectrics with a real permittivity of  $\epsilon_d = 1.96$ . Comparable with some typical materials employed for photosensing in the mid-IR and THz regime, such as  $\text{Hg}_{1-x}\text{Cd}_x\text{Te}$  ternary alloy, the ultrathin light-absorbing semiconductor is modeled through a complex permittivity of  $\epsilon_a = \epsilon' + i\epsilon''$ , where  $\epsilon' = 10.9$  and  $\epsilon''$  is related to the absorption coefficient  $\alpha = 0.1 \mu\text{m}^{-1}$  accounting for the losses[24].

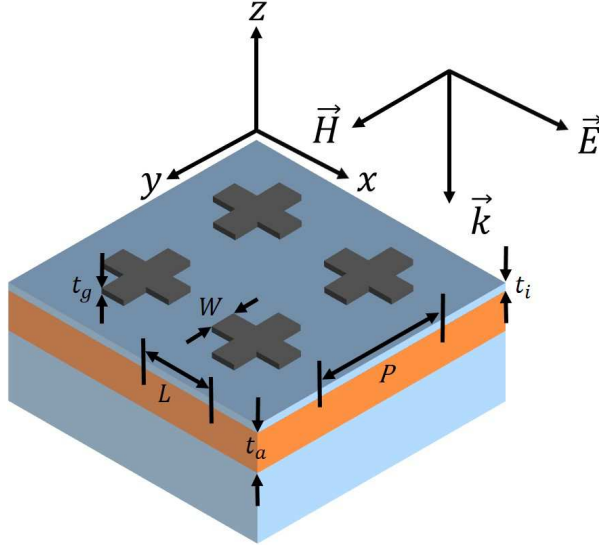


Fig. 1: The schematic geometry of our proposed hybrid periodic array. Each unit cell is composed of a cross-shaped graphene resonator on the top of the light-absorbing semiconductor separated by an insulating spacer.

Graphene is considered as an anisotropic material: isotropic in the plane of sheet and non-dispersive out of the plane, whose permittivity can be described with a diagonal tensor. The in-plane component is  $\epsilon_{xx} = \epsilon_{yy} = 2.5 + i\sigma_g/(\epsilon_0\omega t_g)$ , and the out-of-plane component is  $\epsilon_{zz} = 2.5$ [25,26,27], where  $\epsilon_0$  is the permittivity of vacuum, and  $\omega$  is the angular frequency of the incidence light.  $\sigma_g = ie^2 E_F/[\pi\hbar^2(\omega + i/\tau)]$  is the intraband Drude-like surface conductivity of graphene within the random-phase approximation (RPA)[28, 29], where  $e$  is the charge of an electron,  $E_F$  is the Fermi energy of graphene, and  $\hbar$  is the reduced Planck's constant.  $\tau = \mu E_F/(ev_F^2)$  is the relaxation time, which depends on the electron mobility  $\mu \approx 10000 \text{ cm}^2/\text{Vs}$ , the Fermi energy  $E_F$  and the Fermi velocity  $v_F \approx 10^6 \text{ m/s}$ . To manipulate the Fermi

energy of graphene, similar to that used in Ref. [30,31], the top gate configuration is included (not shown in FIG. 1), and a 100 nm thick ion-gel layer is coated on the top of graphene, which is described by a non-dispersive permittivity  $\varepsilon_{ig} = 1.82$ . The numerical simulations are further performed by using finite-difference time-domain (FDTD) method. The anti-symmetric and symmetric boundary conditions are respectively employed in the  $x$  and  $y$  directions throughout the calculations except when studying the angle polarization tolerance, and perfectly matched layer (PML) boundary conditions are utilized in the  $z$  direction along the propagation of the incidence plane wave[32,33].

### 3 Simulation results and discussions

Cross-shaped graphene resonator is a typical electric ring resonator, which strongly couples to the electric field of the incidence light. The resonance condition reads  $2\pi n_{eff}L/\lambda_{res} = m\pi - \phi$ [34], where  $n_{eff}$  is the effective index depending on the geometric parameters of the structure and the Fermi energy of graphene,  $m=1,2,3, \dots$  accounts for the order of the resonance, and  $\phi$  is the phase change (modulus  $\pi$ ) due to the reflection at the edges of the cross-arm. As the incidence wavelength is much larger than the length of the cross-shaped resonator, only the dipole resonance ( $m=1$ ) is expected to survive. The simulated spectra with an initial Fermi energy of graphene  $E_F = 0.6$  eV are illustrated in FIG. 2. At the resonance around 16  $\mu\text{m}$ , the transmission is strongly suppressed and the absorption is significantly enhanced. The total absorption of the hybrid structure is  $A = 38.8\%$  and the absorption in the light-absorbing semiconductor is  $A' = 22.4\%$ . Note that this ultrathin semiconductor is set to only 100 nm thick with the absorption coefficient  $\alpha = 0.1 \mu\text{m}^{-1}$ , corresponding to an extremely weak absorption of 2% in the impedance matched media, a tenfold absorption enhancement is realized at the resonance.

In view of the theory of plasmonic metamaterials, the enhanced absorption performance in the light-absorbing semiconductor should be attributed to graphene SPR: the localized collective electronic excitations lead to light trapping and field enhancement surrounding the cross-shaped graphene resonator, and thus serve to enhance the light-matter interaction. Based on such consideration, the electric field distributions are essentially analyzed in FIG. 3. At the resonance, a strong enhancement of the  $x$ - $y$  plane electric field ( $|E_z|$ ) is illustrated in FIG. 3a and it mostly concentrates on the edges of the cross-arm along the  $x$  axis. This is a characteristic behavior of the electric dipole resonance in the cross-shaped resonator, which results from the accumulated charges at the edges. More notably, the  $x$ - $z$  cross plane electric field ( $|E_y|$ ) in FIG. 3b clearly shows this plasmon-induced field enhancement extends to the surrounding region. Therefore, such strong resonance can effectively trap the light energy and provide sufficient time to dissipate it by the Ohmic losses in the light-absorbing semiconductor. In contrast, as illustrated in FIG. 3c and 3d, there is nearly no field enhancement for enhanced absorption in the

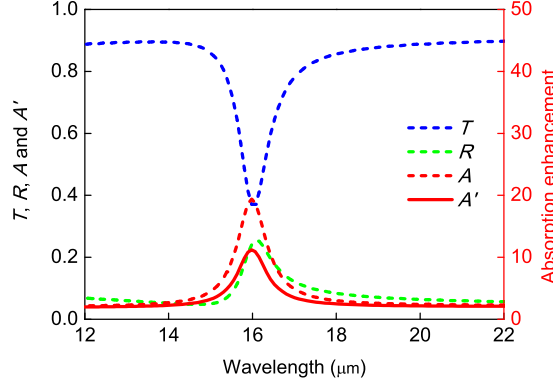


Fig. 2: The simulated transmission  $T$ , reflection  $R$  and absorption  $A$  as well as the absorption in the light-absorbing semiconductor  $A'$  with the Fermi energy of graphene  $E_F = 0.6$  eV. The enhancement factor of absorption in the light-absorbing semiconductor is also shown compared to that in the impedance matched media.

light-absorbing semiconductor at 20  $\mu\text{m}$  since this wavelength is far away from graphene SPR wavelength.

When dealing with a photosensing issue, it is necessary to further examine the photogeneration rate. In the light-absorbing semiconductor, the absorption per unit volume can be calculated from the divergence of the Poynting vector  $P_{abs} = -0.5\text{real}(\nabla \cdot \mathbf{P})$ , which however tends to be very sensitive to numerical calculations. Fortunately, it can be converted to a more numerically stable expression  $P_{abs} = -0.5\omega|E|^2\text{imag}(\varepsilon_a)$ . And the number of absorbed photons per unit volume can then be calculated by dividing by the energy per photon  $g = -0.5|E|^2\text{imag}(\varepsilon_a)/\hbar$ , in proportion to the square of the absolute value of the normalized local electric field  $|E|^2$ . Therefore, the strong electric field enhancement due to graphene SPR can provide a considerably high photogeneration rate. The photogeneration rate distribution (in base 10 logarithmic scale) at the resonance is plotted in FIG. 4. It can be seen that the photogeneration rate is largest ( $\sim 10^{37}$ ) neighboring the edges of the cross-arm along the  $x$  axis and gradually becomes smaller toward the bottom of the light-absorbing semiconductor, showing a comparable performance with those in metal-based plasmon-enhanced photosensors[1].

The optical properties of graphene are largely determined by the Fermi energy. To demonstrate the spectral tunability of the proposed photosensor, the effects of the Fermi energy of graphene on the absorption enhancement are simulated in FIG. 5. When  $E_F$  starts at 0.2 eV, the resonance wavelength locates at 27.9  $\mu\text{m}$  and the absorption in the light-absorbing semiconductor is 7.4%. As  $E_F$  increases to 0.8 eV, the resonance shifts to 13.9  $\mu\text{m}$  and the absorption goes up to 26.0%. Finally, with a high Fermi energy of 1.0 eV, the absorption reaches

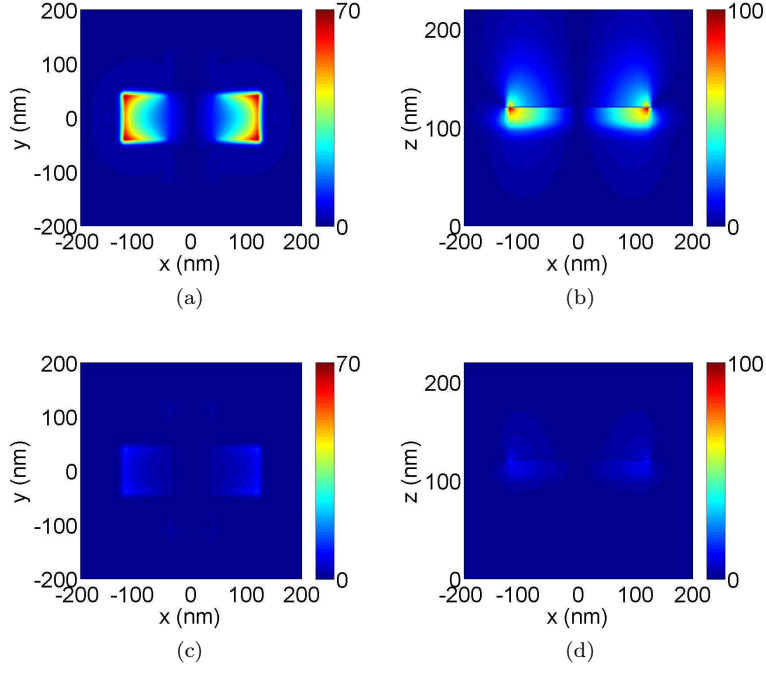


Fig. 3: (a)-(d) The simulated electric field distributions with the Fermi energy of graphene  $E_F = 0.6$  eV. (a)  $|E_z|$  and (b)  $|E_y|$  at the resonance; (c)  $|E_z|$  and (d)  $|E_y|$  at 20  $\mu\text{m}$ .

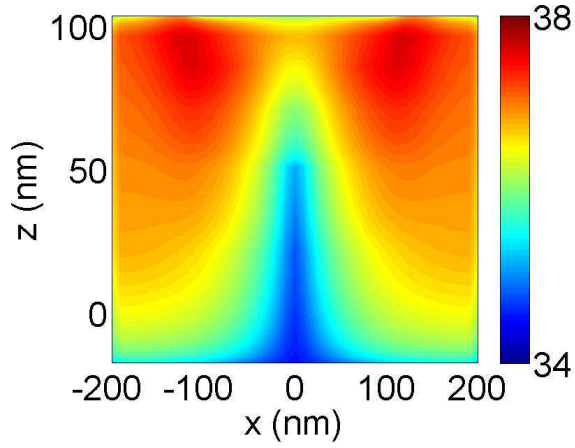


Fig. 4: The simulated photogeneration rate distribution (in base 10 logarithmic scale) with the Fermi energy of graphene  $E_F = 0.6$  eV at the resonance.

28.0% at around 12.4  $\mu\text{m}$ . It can be seen that the resonance experiences a blue shift as the Fermi energy of graphene increases, and the absorption enhancement increases simultaneously. As mentioned above, the resonance wavelength can be described from the resonance condition  $\lambda_{res} = 2\pi n_{eff}L/(\pi - \phi)$ , in positive proportion to the effective index  $n_{eff}$ . Note that  $n_{eff}$  depends largely on the Fermi energy of graphene, and the higher  $E_F$  suggests the smaller  $n_{eff}$ [35,36,37]. Hence the resonance wavelength will become shorter (corresponding to the blue shift of resonance). In the meanwhile, with the increase of the Fermi energy, the conductivity of graphene increases and graphene SPR becomes less lossy, therefore the number of charge carriers contributing to the plasmonic resonance increases. As a result, the field enhancement with higher  $E_F$  are stronger than that with lower  $E_F$ , which leads to a higher absorption enhancement in the light-absorbing semiconductor. As a whole, the tunability of the proposed photosensor with manipulating the Fermi energy of graphene lays the direct foundation for enabling tunable absorption enhancement in the light-absorbing semiconductor without changing the geometric parameters of the structure.

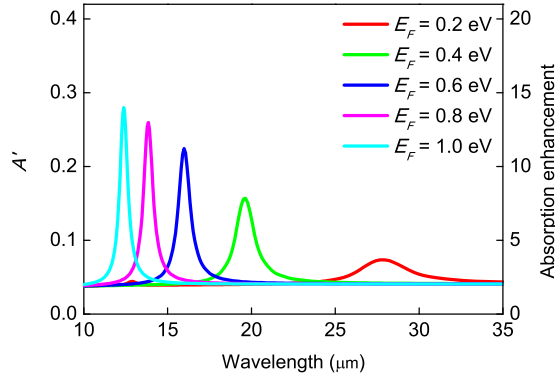


Fig. 5: The simulated absorption in the light-absorbing semiconductor  $A'$  with the Fermi energy of graphene  $E_F$  ranging from 0.2 to 1.0 eV. The enhancement factor of absorption in the absorbing layer is also shown compared to that in the impedance matched media.

The dependences of the absorption in the light-absorbing semiconductor on the incidence angle and polarization are also investigated. As in FIG. 6a and 6b, the resonance wavelength keeps exactly the same and the absorption also remains tenfold enhancement than in the impedance matched media over a large range of incidence angles  $[0^\circ, 45^\circ]$  for both TE and TM polarizations. The good operation angle polarization tolerance is mainly due to the following two reasons: firstly, the cross-shaped graphene resonator possesses the highly

rotational symmetry; secondly, the absorption enhancement here results from the strongly localized surface plasmonic resonance. Consequently, the stable properties of absorption enhancement in the light-absorbing semiconductor is particularly desirable for realizing the robust photosensing platform.

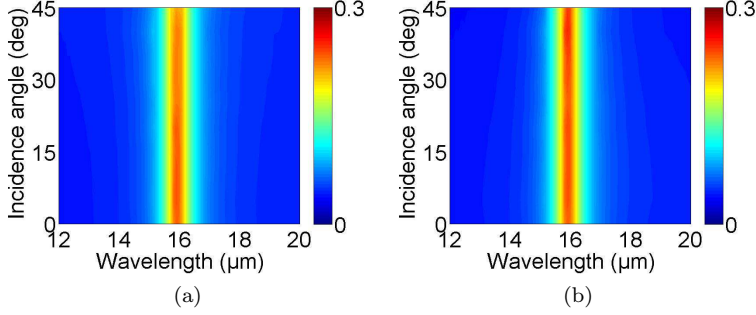


Fig. 6: (a)-(b) The simulated angular dispersions of the absorption in the light-absorbing semiconductor with the Fermi energy of graphene  $E_F = 0.6$  eV for (a) TE and (b) TM configurations.

#### 4 Conclusions

In conclusion, the strong possibility of improving the absorption performance in an ultrathin semiconductor region with graphene SPR is realized in our proposed photosensor. A tenfold absorption enhancement as well as a considerably high photogeneration rate ( $\sim 10^{37}$ ) is demonstrated at the resonance. Moreover, the tunability of graphene SPR with manipulating the Fermi energy enables actively tunable absorption enhancement in the surrounding light-absorbing semiconductor, which can amplify the photoresponse to the incidence light at the selected wavelength and thus be utilized in photosensing with high efficiency and tunable spectral selectivity. Although graphene SPR has mainly been observed in the mid-IR and THz regime, it has also been both theoretically suggested and experimentally demonstrated that graphene SPR can be pushed to much shorter wavelengths ( $\sim 2 \mu\text{m}$ )[14,38], therefore the proposed photosensor together with its design principle can be applied to the near-IR regime.

**Acknowledgements** The author Shuyuan Xiao (SYXIAO) expresses his deepest gratitude to his Ph.D. advisor Tao Wang for providing guidance during this project. SYXIAO would also like to thank Prof. Jianfa Zhang (National University of Defense Technology) for his guidance to the modeling of the light-absorbing semiconductor and Dr. Qi Lin (Hunan University) for beneficial discussion on graphene optical properties. This work is supported by the National Natural Science Foundation of China (Grant No. 61376055,



61006045 and 11647122), the Fundamental Research Funds for the Central Universities (HUST: 2016YXMS024) and the Project of Hubei Provincial Department of Education (Grant No. B2016178).

## References

1. Le Perchec J, Desieres Y, de Lamaestre R E (2009) Plasmon-based photosensors comprising a very thin semiconducting region. *Appl Phys Lett* 94: 181104
2. Knight M W, Sobhani H, Nordlander P, Halas N J (2011) Photodetection with active optical antennas. *Science* 332: 702-704
3. Choi H, Ko S J, Choi Y, Joo P, Kim T, Lee B R, Jung J W, Choi H J, Cha M, Jeong J R, Hwang I W, Song M H, Kim B S, Kim J Y (2013) Versatile surface plasmon resonance of carbon-dot-supported silver nanoparticles in polymer optoelectronic devices. *Nat Photonics* 7: 732-738
4. Wu K, Zhan Y, Wu S, Deng J, Li X (2015) Surface-plasmon enhanced photodetection at communication band based on hot electrons. *J Appl Phys* 118: 063101
5. Luo L B, Zheng K, Ge C W, Zou Y F, Lu R, Wang Y, Wang D D, Zhang T F, Liang F X (2016) Surface Plasmon-Enhanced Nano-photodetector for Green Light Detection. *Plasmonics* 11: 619-625
6. Song S, Chen Q, Jin L, Sun F (2013) Great light absorption enhancement in a graphene photodetector integrated with a metamaterial perfect absorber. *Nanoscale* 5: 9615-9619
7. Cai Y, Zhu J, Liu Q H (2015) Tunable enhanced optical absorption of graphene using plasmonic perfect absorbers. *Appl Phys Lett* 106: 043105
8. Xiong F, Zhang J, Zhu Z, Yuan X, Qin S (2015) Ultrabroadband, More than One Order Absorption Enhancement in Graphene with Plasmonic Light Trapping. *Sci Rep* 5: 16998
9. Guo W, Liu Y, Han T (2016) Ultra-broadband infrared metasurface absorber. *Opt Express* 24: 20586-20592
10. Wang B X, Wang G Z, Wang L L (2016) Design of a novel dual-band terahertz metamaterial absorber. *Plasmonics* 11: 523-530
11. Yi Z, Liu M, Luo J, Zhao Y, Zhang W, Yi Y, Yi Y, Duan T, Wang C, Tang Y (2017) Multiple surface plasmon resonances of square lattice nanohole arrays in Au-SiO<sub>2</sub>-Au multilayer films. *Opt Commun* 390: 1-6
12. Yu H, Zhao Z, Qian Q, Xu J, Gou P, Zou Y, Cao J, Yang L, Qian J, An Z (2017) Metamaterial perfect absorbers with solid and inverse periodic cross structures for optoelectronic applications. *Opt Express* 25: 8288-8295
13. Grigorenko A N, Polini M, Novoselov K S (2012) Graphene plasmonics. *Nat Photonics* 6: 749-758
14. Garcia de Abajo F J (2014) Graphene plasmonics: challenges and opportunities. *ACS Photonics* 1: 135-152
15. Li H J, Wang L L, Liu J Q, Huang Z R, Sun B, Zhai X (2014) Tunable, mid-Infrared ultra-narrowband filtering effect induced by two coplanar graphene strips. *Plasmonics* 9: 1239-1243
16. He X, Gao P, Shi W (2016) A further comparison of graphene and thin metal layers for plasmonics. *Nanoscale* 8: 10388-10397
17. Li H J, Wang L L, Liu J Q, Huang Z R, Sun B, Zhai X (2013) Investigation of the graphene based planar plasmonic filters. *Appl Phys Lett* 103: 211104
18. Lin Q, Zhai X, Wang L, Wang B, Liu G, Xia S (2015) Combined theoretical analysis for plasmon-induced transparency in integrated graphene waveguides with direct and indirect couplings. *EPL* 111: 34004
19. Linder J, Halterman K (2016) Graphene-based extremely wide-angle tunable metamaterial absorber. *Sci Rep* 6: 31225
20. Fu G L, Zhai X, Li H J, Xia S X, Wang L L (2016) Tunable plasmon-induced transparency based on bright-bright mode coupling between two parallel graphene nanostrips. *Plasmonics* 11: 1597C1602
21. Yan X, Wang T, Han X, Xiao S, Zhu Y, Wang Y (2016) High sensitivity nanoplasmonic sensor based on plasmon-induced transparency in a graphene nanoribbon waveguide coupled with detuned graphene square-nanoring resonators. *Plasmonics* at press: <https://doi.org/10.1007/s11468-016-0405-0>

22. Xiao S, Wang T, Jiang X, Yan X, Cheng L, Wang B, Xu C (2017) Strong interaction between graphene layer and Fano resonance in terahertz metamaterials. *J Phys D Appl Phys* at press: <https://doi.org/10.1088/1361-6463/aa69b1>
23. Fang Z, Liu Z, Wang Y, Ajayan P M, Nordlander P, Halas N J (2012) Graphene-antenna sandwich photodetector. *Nano Lett* 12: 3808-3813
24. Rogalski A (2005) HgCdTe infrared detector material: history, status and outlook. *Rep Prog Phys* 68: 2267
25. Gao W, Shu J, Qiu C, Xu Q (2012) Excitation of plasmonic waves in graphene by guided-mode resonances. *ACS Nano* 6: 7806-7813
26. Zeng C, Guo J, Liu X (2014) High-contrast electro-optic modulation of spatial light induced by graphene-integrated Fabry-Prot microcavity. *Appl Phys Lett* 105: 121103
27. Xia S X, Zhai X, Wang L L, Lin Q, Wen S C (2016) Excitation of crest and trough surface plasmon modes in in-plane bended graphene nanoribbons. *Opt Express* 24: 427-436
28. Zhang J, Guo C, Liu K, Zhu Z, Ye W, Yuan X, Qin S (2014) Coherent perfect absorption and transparency in a nanostructured graphene film. *Opt Express* 22: 12524-12532
29. Zhang J, Zhu W, Yuan X, Qin S (2015) Towards photodetection with high efficiency and tunable spectral selectivity: graphene plasmonics for light trapping and absorption engineering. *Nanoscale* 7: 13530-13536
30. Ju L, Geng B, Horng J, Girit C, Martin M, Hao Z, Bechtel H A, Liang X, Zettl A, Shen Y R, Wang F (2011) Graphene plasmonics for tunable terahertz metamaterials. *Nat Nanotechnol* 6: 630-634
31. Hu H, Zhai F, Hu D, Li Z, Bai B, Yang X, Dai Q (2015) Broadly tunable graphene plasmons using an ion-gel top gate with low control voltage. *Nanoscale* 7: 19493-19500
32. Berenger J P (1994) A perfectly matched layer for the absorption of electromagnetic waves. *J Comput Phys* 114: 185-200
33. Berenger J P (2007) Perfectly matched layer (PML) for computational electromagnetics. *Synthesis Lect Comput Electromagnetics* 2: 1-117
34. Ke S, Wang B, Huang H, Long H, Wang K, Lu P (2015) Plasmonic absorption enhancement in periodic cross-shaped graphene arrays. *Opt Express* 23: 8888-8900
35. Li K, Ma X, Zhang Z, Song J, Xu Y, Song G (2014) Sensitive refractive index sensing with tunable sensing range and good operation angle-polarization-tolerance using graphene concentric ring arrays. *J Phys D Appl Phys* 47: 405101
36. Han X, Wang T, Li X, Xiao S, Zhu Y (2015) Dynamically tunable plasmon induced transparency in a graphene-based nanoribbon waveguide coupled with graphene rectangular resonators structure on sapphire substrate. *Opt Express* 23: 31945-31955
37. Xiao S, Wang T, Liu Y, Xu C, Han X, Yan X (2016) Tunable light trapping and absorption enhancement with graphene ring arrays. *Phys Chem Chem Phys* 18: 26661-26669
38. Wang Z, Li T, Almdal K, Mortensen N A, Xiao S, Ndoni S (2016) Experimental demonstration of graphene plasmons working close to the near-infrared window. *Opt Lett* 41: 5345-5348